J. Fluid Mech. (2008), *vol.* 594, *pp.* 369–377.
doi:10.1017/S0022112007008993 Printed in the United Kingdom

The front speed of intrusions into a continuously stratified medium

DIOGO BOLSTER, ALICE HANG AND P. F. LINDEN

Department of Mechanical and Aerospace Engineering, University of California San Diego, La Jolla, CA 92037, USA
dbolster@ucsd.edu

(Received 22 June 2007 and in revised form 1 October 2007)

This paper examines intrusive Boussinesq gravity currents, propagating into a continuously stratified fluid. We develop a model, based on energy arguments, to predict the front speed of such an intrusive gravity current from a lock release. We find that the depth at which the intrusion occurs, which corresponds to the level of neutral buoyancy (i.e. the depth where the intrusion density equals the stratified fluid density), affects the front speed. The maximum speeds occur when the intrusion travels along the top and bottom boundaries and the minimum speed occurs at mid-depth. Experiments and numerical simulations were conducted to compare to the theoretically predicted values, and good agreement was found.

1. Introduction

Gravity currents occur when fluid of one density propagates horizontally into fluid of a different density. Intrusive gravity currents (IGCs) form when a fluid of one density intrudes and travels in a stratified fluid. This may be along a sharp interface between two fluids of different densities, one greater and one less than the intrusion density. Alternatively, the fluid into which the IGC intrudes may be continuously stratified, causing the gravity current to travel along its level of neutral buoyancy (i.e. the height at which the density of the intrusion is the same as that of the ambient fluid).

IGCs along sharp interfaces have been studied extensively. Holyer & Huppert (1980) developed the first theoretical description of IGCs based on mass, momentum and energy conservation in a control volume. The validity of this theory is limited to the case where the interface ahead of the IGC is not deflected. Experimental studies have been conducted by Britter & Simpson (1981), de Rooij, Linden & Dalziel (1999), Lowe, Linden & Rottman (2002) and Sutherland, Kyba & Flynn (2004). Cheong, Kuenen & Linden (2006) developed a model based on energy arguments to predict the front speed of an IGC, even when deflection of the interface does occur.

In this paper we consider the propagation of a Boussinesq high-Reynolds-number intrusion into a continuously stratified fluid. While this type of IGC is similar to an interfacial IGC, there are some fundamental differences. In a continuously stratified fluid internal waves of a different nature to the interfacial wave in a two-layer system can be generated. Some researchers believe that these waves can extract significant energy from the IGC (e.g. Munroe & Sutherland 2006). Experiments which examine bottom-propagating gravity currents in a two-layer fluid (Rottman & Simpson 1989) and a linearly stratified fluid (Maxworthy *et al.* 2002) identified supercritical and

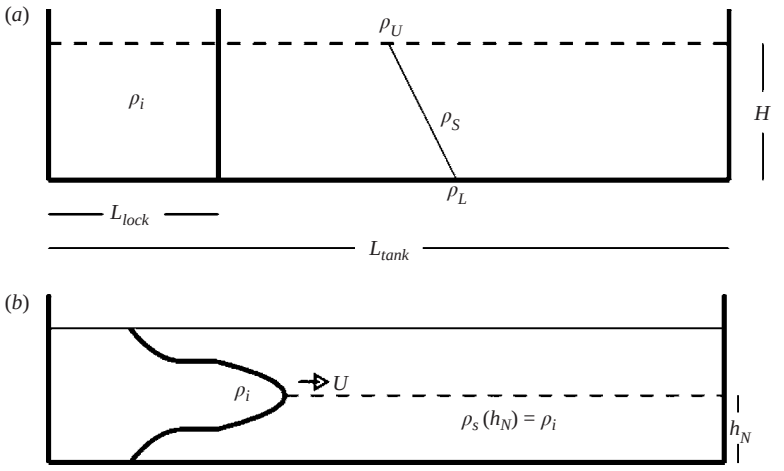

FIGURE 1. (*a*) A schematic of the initial setup for the intrusion where $\rho_U < \rho_i < \rho_L$. (*b*) A schematic of an intruding current with $\rho_i = \frac{1}{2}(\rho_U + \rho_L)$ after the lock has been removed. In this case the neutral level is at $h_N = \frac{1}{2}H$.

subcritical regimes, where the IGC travels faster or slower, respectively, than the fastest internal wave. Cheong *et al.* (2006), who assume perfect conversion of potential energy into kinetic energy of the IGC, and Flynn & Linden (2006), who studied the kinematics of the interfacial wave, suggest that minimal energy is extracted by the wave in the sharp interface case. One issue we address is whether this holds true for the continuously stratified case.

IGCs may be created in the laboratory using a lock release where the density of the intruding fluid ρ_i on one side of the lock lies between the maximum and minimum densities of the stratified fluid, ρ_L and ρ_U, respectively, on the other side of the gate (figure 1). We consider the case where the stratification is uniform and the density of the stratified fluid is given by $\rho_S(z) = \rho_L + (z/H)(\rho_U - \rho_L)$, where H is the depth of the fluid and z is vertically upwards. When the lock gate is removed, the fluid of density ρ_i will travel along its level of neutral buoyancy h_N, where $\rho_S(z = h_N) = \rho_i$.

In the special case where dense fluid propagates along the bottom boundary, the flow corresponds to a dense gravity current. In a uniformly stratified fluid Maxworthy *et al.* (2002) predict that in the early stages after the release the gravity current will travel at a constant velocity U_0 which, from dimensional analysis, takes the form

$$U_0 = FNH, \tag{1.1}$$

where $N = (-g/\rho_0)\,\mathrm{d}\rho/\mathrm{d}z$ is the (constant) buoyancy frequency of the stratification. Here F is a Froude number and ρ_0 is a constant representative density.

In the ideal energy-conserving case Benjamin (1968) showed that, for an ambient fluid of uniform density $F = 0.5$, which matches closely to experimentally measured values of $F = 0.48$. (Shin, Dalziel & Linden 2004). In the stratified case the Froude number is defined as $F = U/[g((\rho_i - \rho_a)/\rho_0)H]^{1/2}$, where ρ_a is the uniform density of the ambient fluid. For boundary currents in a linearly stratified fluid experiments and theoretical work by Maxworthy *et al.* (2002) and Ungarish (2006) suggest values of F of 0.266 and 0.25, respectively. The latter is based on a model that assumes that the relevant density difference driving the current is $\rho_i - \rho_S(z = \frac{1}{2}h)$, corresponding to the average ambient density over the depth of the current. This is equivalent to

defining the Froude number for the uniform ambient case using the average ambient density over the depth of the current. For an energy-conserving current $h = \frac{1}{2}H$, and so $\rho_i - \rho_U = 4(\rho_i - \rho_S(\frac{1}{2}h))$ when $\rho_i = \rho_L$. Thus the factor of 4 is incorporated in (1.1), leading to a reduction in F by a factor of 2. The experimental value of 0.266 found by Maxworthy *et al.* (2002) is in reasonable agreement with this argument.

In this paper we seek to extend this result to an intrusion propagating at any depth in a uniformly stratified fluid. In particular, we wish to determine how the speed of the IGC depends on ρ_i (or equivalently h_N). We present a prediction of the intrusion speed based on an energy argument in § 2. We describe laboratory experiments and two-dimensional numerical simulations in § 3 and compare the results with the theory in § 4.

2. Model

We consider the flow generated when the lock is removed from the system depicted in figure 1. There is a hydrostatic pressure imbalance between the lock and stratified fluid, causing the lock fluid to intrude into the stratified fluid. The resulting exchange flow looks similar to that depicted in figure 1(*b*), where the lock fluid intrudes to the right and there is backflow above and below the intrusion. The intrusion accelerates from rest and then propagates with a constant velocity U. The goal of this work is to predict this constant speed of the intrusion. At later times we expect the intrusion to decelerate, but that phase is beyond the scope of this paper.

In lock-exchange experiments IGCs form as a result of potential energy stored in the original lock configuration. Therefore, in the spirit of Cheong *et al.* (2006), we consider an energy model to predict the front speed U for the uniformly stratified case.

The available potential energy per unit area E due to the horizontal density difference, taking the level of zero buoyancy h_N of the intrusion as the reference level, is

$$\begin{aligned} E &= g\int_{-h_N}^{0}(\rho_S - \rho_i)z'\,\mathrm{d}z' + g\int_{0}^{H-h_N}(\rho_i - \rho_S)z'\,\mathrm{d}z', \\ &= \tfrac{1}{3}\big((\rho_L - \rho_i)gh_N^2 + (\rho_i - \rho_U)g(H-h_N)^2\big). \end{aligned} \tag{2.1}$$

Note here that, taking the intrusion height as the reference height, $-h_N < z' < H - h_N$ and so $\rho_S(z') = \rho_i + (z'/h_N)(\rho_i - \rho_L)$. We define the equilibrium depth, h_E, as the depth of minimum available potential energy, i.e.

$$\left.\frac{\mathrm{d}E}{\mathrm{d}h_N}\right|_{h_N = h_E} = 0. \tag{2.2}$$

It is straightforward to show from (2.1) that

$$h_E = \tfrac{1}{2}H, \tag{2.3}$$

so that the case shown in figure 1(*b*), with $h_N = \frac{1}{2}H$, corresponds to the IGC with minimum available potential energy. Yih (1965) suggested that the kinetic energy of gravity currents and intrusions comes entirely from the conversion of the available potential energy as the density field adjusts. The results of Cheong *et al.* (2006) suggest that this is a good assumption for IGCs along a sharp interface in a two-layer fluid. In this spirit, we assume that a perfect conversion of energy takes place for IGCs in continuously stratified fluids.

Since the minimum potential energy occurs at the mid-depth of the channel, we expect the slowest propagating IGC to occur at this height, with the fastest intrusions being boundary currents. Hence we choose a quadratic form for the intrusion velocity

$$U^2 = U_E^2 \left(a \left(\frac{(h_N - h_E)}{H} \right)^2 + b \left(\frac{(h_N - h_E)}{H} \right) + c \right), \tag{2.4}$$

where U is the speed of the intrusion, U_E is the speed of the intrusion at the equilibrium height h_E and a, b and c are the constant coefficients of the quadratic. This quadratic form is motivated by the quadratic dependence of available potential energy in (2.1) on h_N, along with the assumption that kinetic energy scales on available potential energy.

For Boussinesq currents, symmetry implies that the gravity currents propagating along the top and bottom boundaries will travel at the same speed, implying that $b = 0$. Also, by definition the velocity of the intrusion at the equilibrium height h_E is the equilibrium speed U_E, which gives $c = 1$. In order to close this system we need to find a and U_E.

To do so we use the result (1.1). By symmetry, the intrusion at the mid-depth may be considered as two boundary propagating currents, travelling in a stratified medium of depth $\frac{1}{2}H$. Hence, the speed of the equilibrium intrusion is

$$U_E = \tfrac{1}{2} FNH = \tfrac{1}{2} U_0. \tag{2.5}$$

Thus the IGC at the centre of the channel travels at exactly half the speed of the boundary propagating currents and this condition determines a. Therefore, from (2.3),

$$U = \frac{1}{2} FNH \left(12 \left(\frac{h_N - \frac{1}{2}H}{H} \right)^2 + 1 \right)^{1/2}. \tag{2.6}$$

3. Experiments and numerics

3.1. *Numerics*

For an incompressible Boussinesq fluid of uniform viscosity ν in two dimensions in the (x, z)-plane, the governing equations are

$$\nabla \cdot \boldsymbol{u} = 0, \tag{3.1}$$

$$\frac{\mathrm{D}u}{\mathrm{D}t} = -\frac{1}{\rho_0} \frac{\partial P}{\partial x} + \nu \nabla^2 u, \tag{3.2}$$

$$\frac{\mathrm{D}w}{\mathrm{D}t} = -\frac{1}{\rho_0} \frac{\partial P}{\partial z} - \frac{g\rho'}{\rho_0} + \nu \nabla^2 w, \tag{3.3}$$

$$\frac{\mathrm{D}\rho}{\mathrm{D}t} = \frac{\nu}{Sc} \nabla^2 \rho, \tag{3.4}$$

where $\boldsymbol{u} = (u, w)$ is the velocity, g is gravitational acceleration, ρ_0 is a characteristic reference density, P is the hydrostatically adjusted pressure, Sc is the Schmidt number, $\rho(x, z, t)$ is the fluid density, ρ' is a perturbation from the average background density.

For the simulations reported here, $\nu = 0.01\,\mathrm{cm^2\,s^{-1}}$ and $Sc = 1$. For salt water $Sc = \nu/\kappa \gg 1$ where κ is the diffusivity of salt and, although the choice of $Sc = 1$ leads to a significant overestimation for the diffusivity of salt, this choice is necessary to maintain numerical stability and does not lead to significant changes in the dynamics of the flow (Maxworthy *et al.* 2002; Ungarish & Huppert 2002).

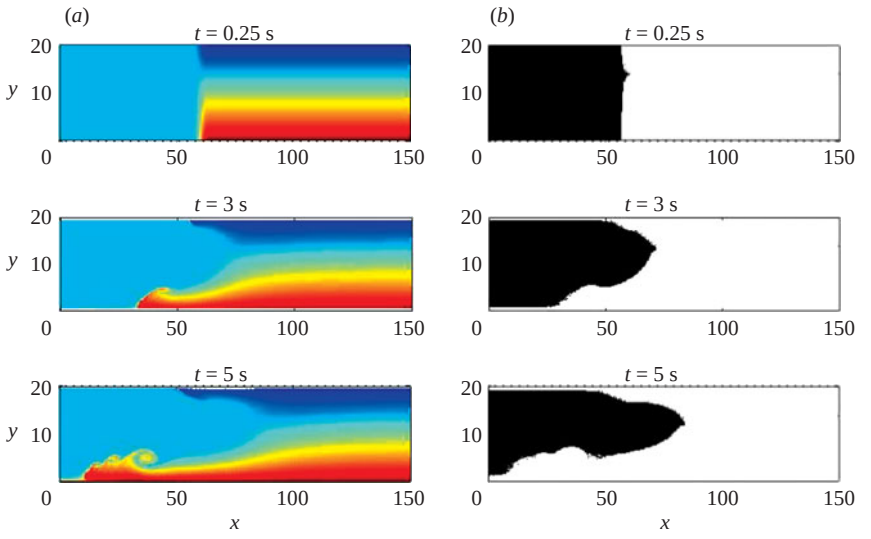

FIGURE 2. Image of an IGC from the numerical solution. (*a*) The stratified field with blue corresponding to the lightest fluid and red corresponding to the densest. (*b*) The intrusion fluid is shown in black. In this case $N = 1$ and $h_N = 0.7$. A comparison of the panels in (*a*) shows that the isopycnal surfaces are deflected downwards by the motion of the intrusion.

A slightly modified version of the open source DNS algorithm Diablo (full details available at http://renaissance.ucsd.edu/fccr/software/Diablo.html) was used to solve the above equations. The code in its current form requires periodic boundary conditions in the streamwise direction. Clearly the flow here is not periodic in the x-direction, and in order to achieve periodicity to enable a Fourier decomposition of the flow variables in this direction a domain twice the length of the domain shown in figure 1 was chosen. This allows a reflectional symmetry about the mid-plane in the initial condition (Sutherland, Flynn & Dohan 2004), i.e. lock fluid starts in the middle and propagates equally in both directions from the middle. In the wall-normal direction periodicity does not occur. Derivatives in this direction were evaluated using centred finite differences with no-slip boundary conditions at the top and bottom boundaries.

A mixed method using a third-order, low-storage Runge–Kutta–Wray (RKW3) and a Crank–Nicholson (CN) scheme was used to advance the flow in time with $\Delta t = 0.001$ s (Bewley 1999; Bewley, Moin & Temam 2001). Diffusive terms in the wall-normal direction were treated implicitly, while all other terms were treated explicitly. Uniform grids were selected in all directions.

As with the laboratory experiments, the flow is stationary at $t = 0$. In order to minimize Gibbs phenomena in the streamwise direction, the vertical interfaces that define the lateral boundaries of the lock are smoothed using a hyperbolic tangent profile, the effect of which can be seen in the density contours in figure 2 at $t = 0.25$ s.

The layer densities are chosen such that the Reynolds number, $Re = NH^2/\nu$, is sufficiently large (i.e. $>10^4$) that viscous effects are negligible and the flow exhibits the characteristic features of two-dimensional turbulent gravity currents such as the roll-up of Kelvin–Helmholtz billows behind the gravity current head. Simulations were carried out for $N = \frac{1}{2}$, $1/\sqrt{2}$ and 1.

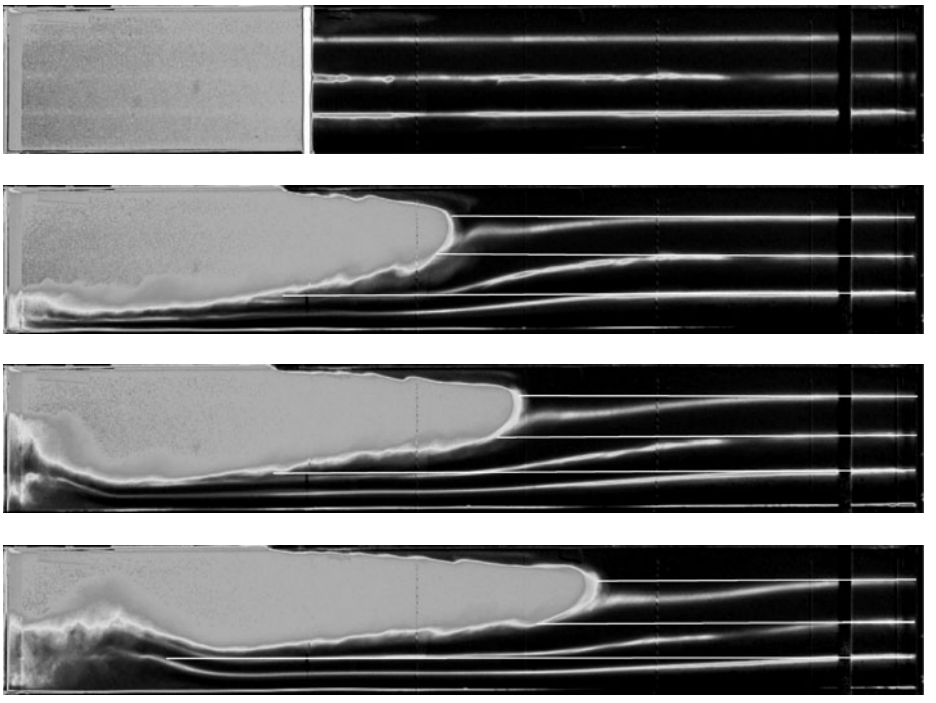

FIGURE 3. Image of an IGC from experiments. In this case $N = 1$ and $h_N = 0.8H$. Note that the isopycnal surfaces, marked with flourescent dye, are deflected downwards ahead of the intrusion. The dye layers in the ambient (right) side of the tank are initially located at intervals of $h/H = 0.25$, 0.5 and 0.75. The original heights of the dye layers are shown by the thin horizontal solid white lines in order to illustrate the induced displacement.

3.2. *Experiments*

The experimental tank was 182 cm long, 23 cm wide and 30 cm deep. For all experiments the total fluid height $H = 20$ cm and the gate was positioned at $L_{lock} = 30$ cm from the endwall (figure 1*a*). Thus the intrusions propagated about 5 lock lengths and so were expected, and observed, to travel at constant speeds after the initial acceleration from rest. The flow was recorded with a CCD camera, connected to a PC for image analysis, and positioned 3.4 m in front of the tank. The back of the tank was covered with tracing film and illuminated with two 95 W fluorescent lamps.

The stratified fluid was produced by the double-bucket method (Oster 1965). The linear stratification was verified with a conductivity probe. The experiment was started by pulling the gate vertically out of the tank. The flow images were captured by the camera every 1/24 s, and analysed using DigiFlow (Dalziel 2004); see figure 3 for an example. The attenuation of light passing through the tank was used to determine the density field in the flow. From this density field, the cross-tank mean density, integrated vertically in the z-direction, was calculated for every x-position and time t. The front speed of the intrusive gravity current was calculated from the resulting x–t plot (for further details of this method see Shin *et al.* 2004).

4. Results

After an initial acceleration from rest, the intrusions were observed to travel at constant speeds until they reached the end of the tank. The results for the intrusion

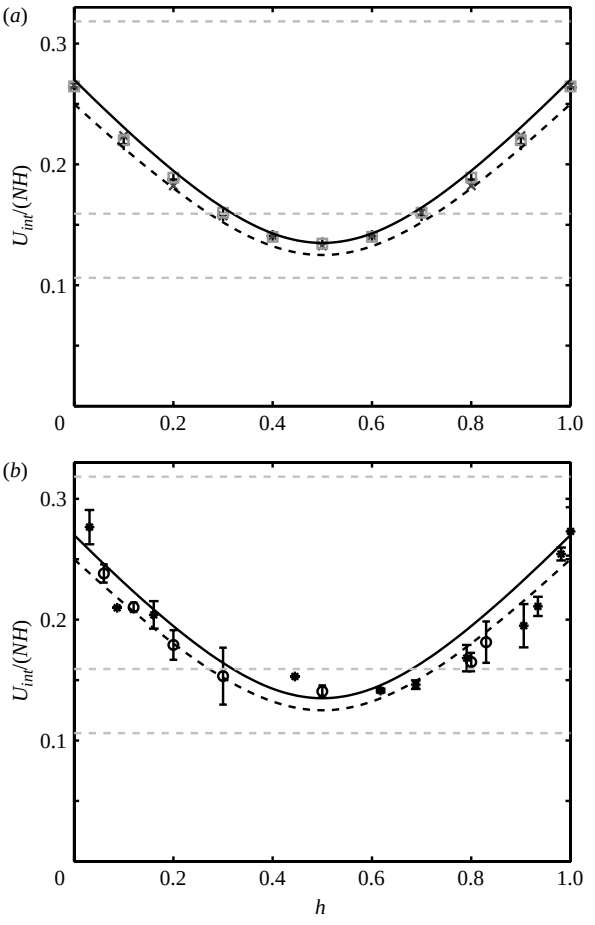

FIGURE 4. Comparison of dimensionless intrusion velocity (U/NH) for (a) numerical simulations and (b) experiments to model predictions. theory $F = 0.266$ (–), Theory $F = 0.25$(– –), experiments (○, $N^2 = 1\,\mathrm{s}^{-2}$; ⋆, $N^2 = \frac{1}{4}\,\mathrm{s}^{-2}$) and numerical predictions (×, $N^2 = 1\,\mathrm{s}^{-2}$; +, $N^2 = \frac{1}{2}\,\mathrm{s}^{-2}$; □, $N^2 = \frac{1}{4}\,\mathrm{s}^{-2}$). The light grey horizontal dashed lines on each plot represent from top to bottom the first-, second- and third-mode long-wave speed respectively.

front speed of the numerical simulations and experiments are shown and compared to the theoretical prediction in figure 4. Two theoretical curves are shown, corresponding to (2.6) for $F = 0.266$ and $F = 0.25$ as discussed above.

The numerical results depicted in figure 4(a) collapse over the range of $N^2 = 0.25 - 1\,\mathrm{s}^{-2}$ over the entire range $0 \leqslant h_N \leqslant H$. Additionally, they agree well with the values predicted from (2.6), lying between the two theoretical curves, suggesting that the energy model presented here is accurate.

The experimental results, while not as close in agreement with the theory as the numerical ones, also collapse and compare favourably. The discrepancies with the experimental results probably stem from the initial condition. In the experiments, the removal of the lock gate generates some vorticity and mixing between the lock and ambient fluid, which is not present in the numerical simulations and appears to affect the current in a non-negligible manner. This effect of the initial condition has been observed in other gravity current work (e.g. Patterson *et al.* 2006), and we observe a

consistent asymmetry with currents in the upper half of the tank ($h_N < \frac{1}{2}H$) travelling slower than expected.

Internal gravity waves were generated in the experiments and numerical simulations (figures 2 and 3). The wave speed for a long wave with vertical mode number n is $NH/n\pi$ and these speeds are shown in figure 4 for $n = 1$, 2 and 3. Thus all intrusions are subcritical with respect to mode-1 waves, subcritical to mode-2 waves for $0.27 < h_N < 0.73$ and supercritical for all higher modes, irrespective of h_N. The fluid ahead of the intrusion is deflected by mode-1 waves for all h_N and mode-2 waves over a limited range of h_N centred at mid-depth. We acknowledge that the observed internal waves have finite horizontal wavelength; however, the long-wave speeds provide upper bounds on the wave speeds and, therefore, on the supercriticality of the intrusion.

5. Conclusion

In this paper we consider Boussinesq intrusive gravity currents, intruding into a continuously stratified fluid with constant buoyancy frequency N. We conduct lock release experiments where fluid of intermediate density intrudes into the stratified ambient fluid. The fluid will intrude at height h_N, its level of neutral relative buoyancy. The goal was to predict the speed of the front of the IGC during the initial phase when it travels at constant speed. We developed a model based on energy arguments and showed that the maximum velocities occur when the current travels along the top and bottom boundaries, with the minimum intrusion velocity occurring when the current travels at mid-depth. The mid-depth velocity is exactly half of the maximum velocity. In order to verify the validity of our model we conducted a full series of numerical and laboratory experiments, where we measured intrusion velocities which displayed good agreement with the values predicted by our model.

These results imply that the role of internal gravity waves generated by the intrusion is subtle. Ungarish & Huppert (2002, 2006) and Ungarish (2005), based on a one-layer shallow water model, illustrate that the energy associated with internal waves for boundary currents is small compared to the available potential energy. Since our model assumes a direct scaling of available potential energy to kinetic energy for all cases and the agreement between model and experiments is good, this suggests that the waves carry little energy for all intrusion heights. A similar conclusion for the energy content of the interfacial wave for an IGC propagating in a two-layer fluid was drawn by Cheong *et al.* (2006).

The fact that the internal waves do not carry much energy does not mean that they do not play an important role in the flow. In fact, Maxworthy *et al.* (2002) and Sutherland & Nault (2007), who discuss the interaction of these waves with the head of the current, illustrate that the role of the waves is important. In the two-layer case, Flynn & Linden (2006) show that the deflection of the interface ahead of the IGC caused by the wave changes the upstream conditions that the current sees. By taking this change into account they were able to modify the Holyer & Huppert (1980) control-volume analysis and obtain accurate predictions for the intrusion speed.

The same mechanism appears to occur in the continuously stratified case. All intrusions are subcritical to mode-1 waves (figure 4) and this mode will be generated whenever $h_N \neq \frac{1}{2}H$, causing a vertical deflection of the upstream conditions. Intrusions with $0.27 < h_N < 0.73$ are also subcritical to mode-2 waves, but the deflections caused by these are asymmetrical about the mid-depth of the channel and so cause only small net displacement of the isopycnals. Thus we expect that a control-volume analysis for

the continuously stratified case which accounts for the changed upstream conditions caused by the mode-1 long internal wave should lead to a prediction for the intrusion speed. This, however, is no trivial task and is left for future work.

REFERENCES

Benjamin, T. B. 1968 Gravity currents and related phenomena. *J. Fluid Mech.* **31**, 209–248.

Bewley, T. R. 1999 Linear control and estimation of nonlinear chaotic convection: harnessing the butterfly effec. *Phys. Fluids* **11**, 1169–1186.

Bewley, T. R., Moin, P. & Temam, R. 2001 DNS-based predictive control of turbulence: an optimal benchmark for feedback algorithms. *J. Fluid Mech.* **447**, 179–225.

Britter, R. E. & Simpson, J. E. 1981 A note on the structure of the head of an intrusive gravity current. *J. Fluid Mech.* **112**, 459–466.

Cheong, H. B., Kuenen, J. J. & Linden, P. F. 2006 The front speed of intrusive gravity currents. *J. Fluid Mech.* **552**, 1–11.

Dalziel, S. B. 2004 Digiflow user manual. *http://www.damtp.com.ac.uk/lab/digiflow*.

Flynn, M. R. & Linden, P. F. 2006 Intrusive gravity currents. *J. Fluid Mech.* **568**, 193–202.

Holyer, J. Y. & Huppert, H. E. 1980 Gravity currents entering a two-layer fluid. *J. Fluid. Mech.* **100**, 739–767.

Lowe, R. J., Linden, P. F. & Rottman, J. W. 2002 A laboratory study of the velocity structure in an intrusive gravity current. *J. Fluid Mech.* **456**, 33–48.

Maxworthy, T., Leilich, J., Simpson, J. & Meiburg, E. H. 2002 The propagation of a gravity current in a linearly stratified fluid. *J. Fluid Mech.* **453**, 371–394.

Munroe, J. R. & Sutherland, B. R. 2006 Intrusions and internal waves in stratified fluids. *Proc. Sixth Intl Symp. on Stratified Flows – Perth* (ed. G. Ivey), pp. 446–451.

Oster, G. 1965 Density gradients. *Sci. Am.* **213**, 70.

Patterson, M. D., Simpson, J. E., Dalziel, S. B. & van Heijst, G. J. F. 2006 Vortical motion in the head of an axisymmetric gravity current. *Physics of Fluid* **18**, 86–97.

de Rooij, F., Linden, P. F. & Dalziel, S. B. 1999 Saline and particle-driven interfacial intrusions. *J. Fluid Mech.* **389**, 303–334.

Rottman, J. W. & Simpson, J. E. 1989 The formation of internal bores in the atmosphere: A laboratory model. *Q. J. R. Metl. Soc.* **115**, 941–963.

Shin, J. O., Dalziel, S. B. & Linden, P. F. 2004 Gravity currents produced by lock exchange. *J. Fluid Mech.* **521**, 1–34.

Sutherland, B. & Nault, J. 2007 Intrusive gravity currents propagating along thin and thick interfaces. *J. Fluid Mech.* **586**, 109–118.

Sutherland, B. R., Flynn, M. R. & Dohan, K. 2004 Internal wave excitation from a collapsing mixed region. *Deep Sea Res.* II **51**, 2889–2904.

Sutherland, B. R., Kyba, P. J. & Flynn, M. R. 2004 Intrusive gravity currents in two-layer fluids. *J. Fluid Mech.* **514**, 327–353.

Ungarish, M 2005 Intrusive gravity currents in a stratified ambient: shallow-water theory and numerical results. *J. Fluid Mech.* **535**, 287–323.

Ungarish, M. 2006 On gravity currents in a linearly stratified ambient: a generalization of Benjamin's steady-state propagation results. *J. Fluid Mech.* **548**, 49–68.

Ungarish, M. & Huppert, H. E. 2002 On gravity currents propagating at the base of a stratified fluid. *J. Fluid Mech.* **458**, 283–301.

Ungarish, M. & Huppert, H. E. 2006 Energy balances for propagating gravity currents: homogenous and stratified ambients. *J. Fluid Mech.* **565**, 363–380.

Yih, C. S. 1965 *Dynamics of Nonhomogenous Fluids.* MacMillan.